AD-A164 574 STABILITY AND PROPERTIES OF COMPOSITIONALLY MODULATED FILMS(U) HARVARD UNIV CAMBRIDGE MA DIV OF APPLIED SCIENCES R C CAMMARATA ET AL. NOV 85 TR-28 1/1

UNCLASSIFIED N00014-85-K-0023 F/G 20/12 NN

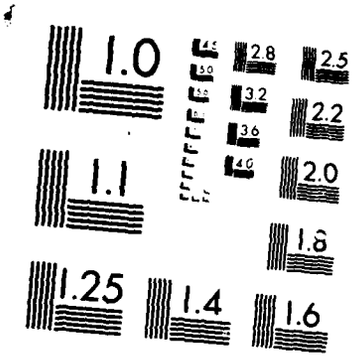

(8)

Office of Naval Research

Contract Number N00014-85-K-0023

STABILITY AND PROPERTIES OF COMPOSITIONALLY MODULATED FILMS

Technical Report No. 28

by

R.C. Cammarata, S.M. Prokes and F. Spaepen

November 1985

Division of Applied Sciences
Harvard University
Pierce Hall, 29 Oxford Street
Cambridge, Massachusetts 02138

Unclassified

SECURITY CLASSIFICATION OF THIS PAGE (When Data Entered)

REPORT DOCUMENTATION PAGE		READ INSTRUCTIONS BEFORE COMPLETING FORM
1. REPORT NUMBER Technical Report No. 28	2. GOVT ACCESSION NO. AD A164 574	3. RECIPIENT'S CATALOG NUMBER
4. TITLE (and Subtitle) STABILITY AND PROPERTIES OF COMPOSITIONALLY MODULATED FILMS		5. TYPE OF REPORT & PERIOD COVERED Interim Report 6. PERFORMING ORG. REPORT NUMBER
7. AUTHOR(s) R.C. Cammarata, S.M. Prokes, F. Spaepen		8. CONTRACT OR GRANT NUMBER(s) N00014-85-K-0023
9. PERFORMING ORGANIZATION NAME AND ADDRESS Division of Applied Sciences Harvard University Cambridge, MA 02138		10. PROGRAM ELEMENT, PROJECT, TASK AREA & WORK UNIT NUMBERS
11. CONTROLLING OFFICE NAME AND ADDRESS		12. REPORT DATE November 1985 13. NUMBER OF PAGES
14. MONITORING AGENCY NAME & ADDRESS (if different from Controlling Office)		15. SECURITY CLASS. (of this report) Unclassified 15a. DECLASSIFICATION/DOWNGRADING SCHEDULE

16. DISTRIBUTION STATEMENT (of this Report)

This document has been approved for public release and sale; its distribution is unlimited. Reproduction in whole or in part is permitted by the U.S. government.

17. DISTRIBUTION STATEMENT (of the abstract entered in Block 20, if different from Report)

18. SUPPLEMENTARY NOTES

19. KEY WORDS (Continue on reverse side if necessary and identify by block number)

compositionally modulated films, multilayers, superlattices, interdiffusion, amorphous Si, amorphous Ge, coarsening, layer stability, supermodulus effect, coherency stress, Fermi surface, Brillouin zone, modulus enhancement

20. ABSTRACT (Continue on reverse side if necessary and identify by block number)

The thermodynamics and kinetics governing the stability of compositionally modulated materials are reviewed. Typical results of experiments on fcc and amorphous metals are presented to demonstrate the effects of interdiffusion. Two coarsening mechanisms are analyzed, as is the stability of orthogonal waves in phase separating systems.

The interdiffusivity between amorphous Si and Ge in the temperature range 550-630K is $1.07 \times 10^{-10} \exp(-1.6 \text{ ev/kT}) m^2 s^{-1}$, for a modulation wavelength of

-- continued --

DD FORM 1 JAN 73 1473 EDITION OF 1 NOV 65 IS OBSOLETE
S/N 0102-014-6601

Unclassified

SECURITY CLASSIFICATION OF THIS PAGE (When Data Entered)

5.83 nm. No crystallization occurred during the anneals.

The theories for the enhancement of the elastic modulus in crystalline compositionally modulated films are reviewed. Both the Fermi sphere-Brillouin zone interaction model and the coherency stress model are found to be inadequate and insufficiently developed.

PREFACE

This report contains three recent papers on the stability and properties of compositionally modulated films.

INTERDIFFUSION AND STABILITY OF COMPOSITIONALLY MODULATED FILMS

Frans SPAEPEN*
Division of Applied Sciences, Harvard University, Cambridge, MA 02138

ABSTRACT

The thermodynamics and kinetics governing the stability of compositionally modulated materials are reviewed. Typical results of interdiffusion experiments on fcc and amorphous metals are discussed to demonstrate the sensitivity and special features of the technique. Two coarsening mechanisms, and the stability of orthogonal waves in phase separating systems are analyzed.

INTRODUCTION

Compositionally modulated materials are produced by multiple alternate deposition of very thin layers of different composition. The deposition methods include vapor deposition [1,2], molecular beam epitaxy [3], sputtering [4,5], and chemical vapor deposition [6]. If a structure has a reasonably low free energy over an extended continuous composition range, and if there is sufficient intermixing during the deposition process, the multiple layering process can result in the formation of a compositionally modulated material, i.e. one in which the composition profile is closely approximated by a simple harmonic function :

$$c = c_0 + A \cos \beta x \qquad (1)$$

where c_0 is the average composition, x the distance coordinate normal to the film plane, A the modulation amplitude and β the modulation wavenumber ($\beta = 2\pi/\lambda$; λ is the modulation wavelength). Of interest here are materials with λ between 0.2 and 10 nm. This composition modulation can be measured by X-ray diffraction [7,8]. It gives rise to a peak at $\vec{k} = \beta\vec{x}$, with intensity proportional to A^2. This peak can be considered as a satellite of the (000) forward scattering peak, and is independent of the atomic scale structure (crystalline or amorphous) of the material. In crystalline materials, satellites also appear at $\vec{k}_{hkl} \pm \beta\vec{x}$ around the higher order Bragg peaks (hkl); their intensity, however, is not just dependent on A^2, but also on the variation in lattice spacing. Deviations from a simple harmonic composition modulation (eq. (1)) can be detected from the higher order peaks at $\vec{k} = n\beta\vec{x}$, (n = 2, 3, ...).

Crystalline compositionally modulated metallic films have been made most successfully in binary fcc systems with full solid solubility. For example : Ag-Cu [2], Cu-Pd [9], Au-Ni [10], Au-Cu [11] and Cu-Ni[12,13]. Usually a mica substrate was used, which produced films with a strong (111) texture that were fully coherent for small enough wavelength.

Amorphous compositionally modulated metallic films have so far only been reported for metal-metalloid alloys, such as $(Pd_{85}Si_{15})$ - $(Fe_{85}B_{15})$ [5, 14-16]. Modulated binary amorphous systems have only very recently been obtained; for example Cu-Zr [17-18] and Ni-Zr [18]. These amorphous modulated films differ in important ways from the crystalline ones :

---

* Visiting Professor, Metallurgy Department, University of Leuven, Belgium, Fall 1984-1985.

Mat. Res. Soc. Symp. Proc. Vol. 37 ©1985 Materials Research Society

(i) They can be produced at any value of λ, without interference between the periodicity of the atomic structure, as is the case at short modulation wavelengths in crystals. Because the spatial distribution of atom centers in an amorphous system is continuous and the composition c in equation (1) is the average one over the yz-plane at position x, λ can, in principle, be made arbitrarily small. In an X-ray diffractometer experiment with the scattering vector $\vec{k}$ along $\hat{x}$, the same averaging is done, and therefore a peak at an arbitrarily large value of β could be observed. On a *local* scale, however, the composition gradient can not be much greater than 1/a (a : average interatomic distance), even if dc/dx in the averaged equation (1) is very large at small λ. This is important in view of the local composition gradient contributions to the free energy, discussed below. In crystalline materials, the continuum description must be corrected when λ approaches 2a; a similar correction seems required for amorphous materials.
(ii) In many systems, amorphous alloys can be produced over a much larger continuous composition range than their crystalline counterparts. Producing a composition modulation in such a system may therefore only be possible in the amorphous state.
(iii) Coherency strains, which can contribute considerably to the free energy of crystalline modulated films and must be taken into account in the analysis of interdiffusion [9], are absent, presumably at least initially, in amorphous metallic modulated films. They may arise from chemical changes during the interdiffusion process [19].
(iv) Short circuit diffusion paths, especially grain boundaries (see below), are not found in the amorphous films. This simplifies the analysis of the early stages of the interdiffusion, and, from a practical point of view, enhances the stability and useful life of the films.

Artificial compositionally modulated materials described above are thermodynamically unstable. They have an unusually high density of interfaces, which can be eliminated in two ways : homogenization by interdiffusion, or sharpening of the composition profile followed by coarsening. The thermodynamic conditions determining the evolution of a modulated structure will be discussed in Section 2. Monitoring the intensity of the modulation satellites as a function of annealing time is the most sensitive method for measuring interdiffusivity, which is especially useful for the study of amorphous metals; this will be discussed in Section 3. Some mechanisms of coarsening are identified and analyzed in Section 4. A more detailed survey of some of the theory and experiments discussed here can be found in a forthcoming review paper [20].

THERMODYNAMICS

The theory of the thermodynamics and stability of systems, such as the modulated films, that are inhomogeneous on a very fine scale was first fully formulated by Cahn and Hilliard [21-23]. A detailed exposition can be found in the excellent review paper by Hilliard [24]. A review of the historical development was given by Cahn in his 1967 Institute of Metals Lecture [25]. In this section, the most important results are outlined.

In an inhomogeneous system, the free energy of a volume element is not only dependent on the local composition, but also on that of the neighboring volume elements through the formation of interfaces with a composition gradient. For an inhomogeneity in one dimension, $\hat{x}$, the total free energy of the system can then be written as :

$$F = \alpha \int [f(c) + \kappa (\frac{\partial c}{\partial x})^2] \, dx \qquad (2)$$

$c\ell$ is the area perpendicular to $\vec{x}$; f(c) is the free energy per unit volume of a homogeneous system of composition c; κ is the gradient energy coefficient. If F is minimized, under the constraint of conservation of mass the following stability condition is obtained :

$$f' - 2\kappa \frac{\partial^2 c}{\partial x^2} = a \tag{3}$$

where a is a constant if the system is in equilibrium. Note that $f' = (\mu_A - \mu_B)/\bar{V}$ = constant (μ_i : chemical potential of element i, $\bar{V}$: molar volume) is the equilibrium condition for a system with negligible gradient energy. If such a system is not in equilibrium, the gradient of f' becomes the driving force for the interdiffusion flux, $\vec{J}$, towards equilibrium :

$$\vec{J} = - M \frac{\partial f'}{\partial x} \tag{4}$$

where M is the mobility. In the presence of gradient energy contributions, the driving potential for interdiffusion becomes a in equation (3) :

$$\vec{J} = - M \frac{\partial a}{\partial x} \tag{5}$$

Combination of equations (3) and (5) with the conservation of mass, $\partial c/\partial t = - \vec{V} \cdot \mathrm{div}\, \vec{J}$, gives the diffusion equation :

$$\frac{\partial c}{\partial t} = \tilde{D} \left[\frac{\partial^2 c}{\partial x^2} - \frac{2\kappa}{f''} \frac{\partial^4 c}{\partial x^4} \right] \tag{6}$$

where M, f" and κ are assumed constant to obtain a linear equation. The bulk interdiffusion coefficient is :

$$\tilde{D} = M f'' \bar{V} \tag{7}$$

The evolution of a composition modulation wave is obtained by inserting equation (1) in the diffusion equation, which yields :

$$A = \exp \left[- \tilde{D} \beta^2 \left(1 + \frac{2\kappa \beta^2}{f''} \right) t \right] \tag{8}$$

The relative rate of change in amplitude is defined as an amplification factor :

$$R = \frac{1}{A} \frac{\partial A}{\partial t} = - \tilde{D}_\lambda \beta^2, \tag{9}$$

where

$$\tilde{D}_\lambda = \tilde{D} \left(1 + \frac{2\kappa \beta^2}{f''} \right) \tag{10}$$

is the wavelength-dependent interdiffusion coefficient.

The growth or decay of a modulation wave now depends on the sign of R. Three different cases, illustrated on Figure 1, can be distinguished. To facilitate the interpretation it is useful to consider the predictions of the regular solution model for f" and κ. For an equiatomic binary mixture, with a molar energy of mixture ΔU :

$$f'' = \frac{4}{\bar{V}} \left[RT - 2\Delta U \right] \tag{11}$$

The gradient energy coefficient is [21] : $\kappa = \frac{2\, \Delta U\, a^2}{\bar{V}}$ (12)

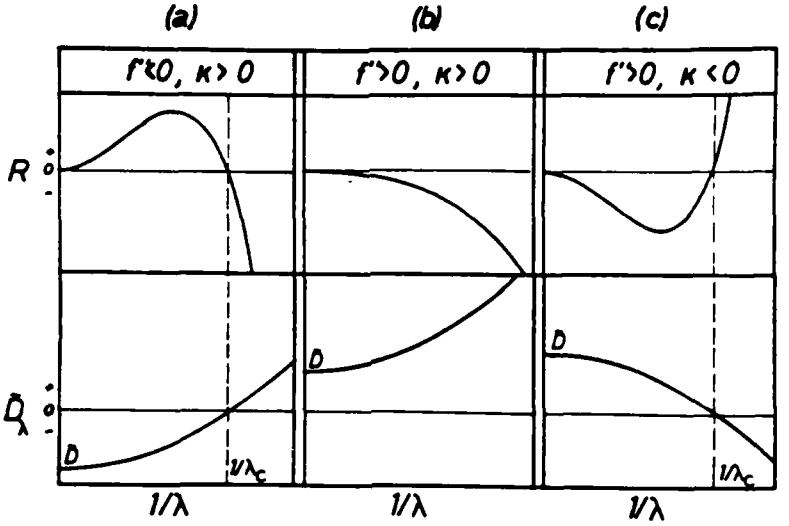

Figure 1 : Dependence of the amplification factor, R, and the interdiffusivity, $\tilde{D}_\lambda$, on the modulation wavelength for a phase separating system inside the spinodal (a), and outside the spinodal (b), and for an ordering system (c).

Figure 1a ($f'' < 0$, $\kappa > 0$) corresponds to a phase separating system ($\Delta U > 0$) inside the spinodal. Modulations with wavelengths greater than $\lambda_c = 2\pi/\beta = 2\pi(-2\kappa/f'')^{1/2}$ grow; this is the classical case of spinodal decomposition, corresponding to uphill diffusion ($\tilde{D} < 0$, eq. (7)). Modulations with $\lambda < \lambda_c$ decay, due to their high density of interfaces which make a positive gradient energy contribution.
Figure 1b ($f'' > 0$, $\kappa > 0$) corresponds to a phase separating system ($\Delta U > 0$) outside the spinodal. The diffusion coefficient is positive for all wavelengths, and increases with decreasing wavelength due to the increasing driving force for homogenization from the interfacial energy. Figure 1c ($f'' < 0$, $\kappa < 0$) corresponds to an ordering system ($\Delta U < 0$), and is the exact negative of Figure 1a. At long wavelengths ($\lambda > \lambda_c$), the system homogenizes ($\tilde{D} > 0$, eq. (7)). Modulations with short wavelength ($\lambda < \lambda_c$) are predicted to grow; since λ_c in crystalline systems is usually on the order of the atomic spacing, the development of very short wavelength "phase separation" can be interpreted as an ordering process. It should also be kept in mind that the continuum approximation used above must break down at small λ. Corrections for the discreteness of the crystalline lattice have been made by Cook et al. [26]. The fourth possibility ($f'' < 0$, $\kappa < 0$) is an unlikely one. In fact, it can not occur in the regular solution approximation (equations (11) and (12)).

Since the lattice parameter of an alloy depends on its composition ($\eta = d(\ln a)/dc$), matching of the lattice planes along a modulation wave introduces coherency strains. The free energy of eq. (2) now acquires an additional term [22,23]:

$$F = \alpha \int \left[f(c) + \kappa \left(\frac{\partial c}{\partial x}\right)^2 + \eta^2 Y (c - c_0)^2 \right] dx \qquad (13)$$

where Y is a modulus that depends on the crystal symmetry and the direction of the modulation wave. For an isotropic continuum [22] :

$$Y = E/(1 - \nu) \tag{14}$$

E : Young's modulus; ν : Poisson's ratio.
As a result, the interdiffusion coefficient now contains an additional positive (i.e. homogenizing) term :

$$\tilde{D}_\lambda = \tilde{D}\left(1 + \frac{2\kappa\beta^2}{f''}\right) + 2M\eta^2 Y \tag{15}$$

Note that f" now must be more negative to cause spinodal decomposition than in the absence of coherency strains. The condition $f'' < -2\eta^2 Y$ defines the "coherent spinodal".

INTERDIFFUSION

Since the intensity, I, of the (000) satellite is proportional to A^2, (as are the (hkl) satellites in the absence of coherency strains) is the slope of a plot of ln I vs t, according to eq. (9), equal to $-2 D_\lambda \beta^2$. Such a plot usually shows an initial transient with a decreasing slope before settling down to a "terminal slope" from which the interdiffusivity is taken. Cook and Hilliard [2] have attributed these transients to increased homogenization in moving grain boundaries as a result of texture-driven grain growth (see Figure 2).

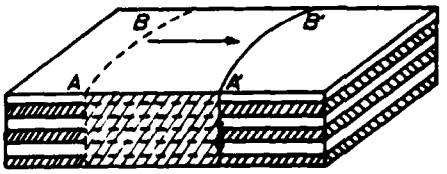

Figure 2 : Schematic diagram of the homogenization by diffusion in a grain boundary moving from AB to A'B'.

In interdiffusion experiments on fcc-metallic compositionally modulated materials, the wavelength dependence of $\tilde{D}_\lambda$ was found to obey equations (10) or (15), and the first direct determinations of the gradient energy coefficient, κ, were made. Cook and Hilliard [2] studied the Ag-Au system, in which the coherency strain effects are negligible (η = 0.15 %). A fit of their data to eq. (10) gave $\kappa = -2.6 \times 10^{-11}$ J.m^{-1}, a negative value as expected for an ordering system (Figure 1c). In the temperature range 200-250°C they measured bulk interdiffusivities, $\tilde{D}$, as low as 10^{-24} m^2.s^{-1}, which were in perfect agreement with an extrapolation of high temperature (> 900°C) data ($\tilde{D} > 10^{-14}$ m^2.s^{-1}), which clearly represent lattice diffusion. The modulated film technique is therefore not only the most sensitive one, but it also allows determination of the lattice diffusivity in a temperature regime ($T < 2T_M/3$) where other techniques would only detect short-circuit diffusion along grain boundaries or dislocations. The reason for this is, of course, that the diffusion distance for lattice diffusion ($\lambda/2$) is much lesser than either the grain size or the distance between dislocations, so that the fraction of the material homogenized by short circuit diffusion is negligible to that homogenized by lattice diffusion. The only short circuit mechanism that can homogenize an appreciable amount of material is that involving moving grain boundaries, as discussed above (see Figure 2). This mechanism also explains the very high effective diffusivities

observed in the earliest compositionally modulated materials [1], which had a fine-grained polycrystalline structure.

The effect of the coherency strain on the diffusivity was confirmed by Philofsky and Hilliard [9] for the Cu-Pd system (η = 7 %). By comparing the intensities of the satellites at $\bar{k}_{111} + \beta$ and $\bar{k}_{111} - \beta$, they established that for full coherence the modulation wavelength had to be less than 2.8 mm; beyond that, a gradual loss of coherence was observed with full incoherence beyond 3.8 mm. The wavelength dependence of $\tilde{D}_\lambda$ was found to obey equation (15) for $\lambda < 2.8$ mm; beyond that a gradual decrease of D_λ with λ was observed, corresponding with the decrease in the positive strain term in equation (15).

The modulated film technique has special advantages in the study of diffusion in metallic glasses.

(i) Since metallic glasses crystallize rapidly if their diffusivity is greater than about 10^{-20} $m^2.s^{-1}$, sensitive detection techniques are required. The solution of all other methods for measuring the diffusivity is determined by the spatial resolution of the "slicing" technique used to analyze a single diffusion junction. Specialized techniques, such as sputter profiling, Rutherford backscattering or nuclear reactions must be used on the metallic glasses, and they are limited to only a few orders of magnitude of D. Below 10^{-23} $m^2.s^{-1}$, only the modulated film technique is available. Its sensitivity is a result of its being composed of several hundred diffusion junctions, so that very small changes in the composition profile, corresponding to a diffusion distance of no more than 10 pm, can be detected by the X-ray technique.

(ii) Since glasses are thermodynamically unstable, they undergo a continuous series of transformations to states of lower free energy. This process of structural relaxation affects all physical properties, but most strongly the atomic transport properties such as viscosity [27] and diffusivity [15]. Since the modulated film technique is non-destructive it can be used conveniently to measure the time dependence of the diffusivity. Metallic glasses show a very large transient in their ln I vs t curve, which can only be attributed to structural relaxation [15]; indeed, for a $(Pd_{85}Si_{15})_{50}/(Fe_{85}B_{15})_{50}$ film, the quantity $\tilde{D}_\lambda^{-1}(t)$ was observed to increase linearly with time, exactly as one would expect from a scaling relation with the viscosity, which has also been observed to increase linearly with annealing time [27]. The technique also allows iso-configurational measurements of the temperature dependence of $\tilde{D}$. After sufficient annealing, structural relaxation becomes slow enough so that upon cycling of the temperature, D can be reproduced. The iso-configurational activation energy for diffusion measured this way was very close to that of the viscosity in a similar system [15,27].

(iii) Since interdiffusion is driven by a chemical driving force, the modulated film technique allows insight into the thermodynamics of metallic glasses, which are difficult to obtain otherwise. Cammerata and Greer [16] have studied the wavelength dependence of D_λ in the $(Pd_{85}Si_{15})_{50}/(Fe_{85}B_{15})_{50}$ system. Their results are redrawn on Figure 3, together with the fit to equation (10). The data points were taken from the terminal slopes of ln I vs t curves. Since the films had identical fabrication and thermal histories, and exhibited similar relaxation kinetics, the data were assumed to correspond to the same degree of relaxation. Nevertheless, part of the scatter in the data may still be due to the difficulty in reproducing an identical structural state. The system is clearly a homogenizing one. Since the bulk interdiffusivity, $\tilde{D}$, is positive, $f'' > 0$ according to equation (7). Since the slope of D_λ vs β is negative, κ must be negative, which, according to the regular solution approximation (equation (12)), corresponds to an ordering system. The equiatomic heat of mixing, ΔU, for Pd and Fe, which are the heaviest elements whose interdiffusion is mainly being observed by the X-ray technique, has indeed been calculated to be

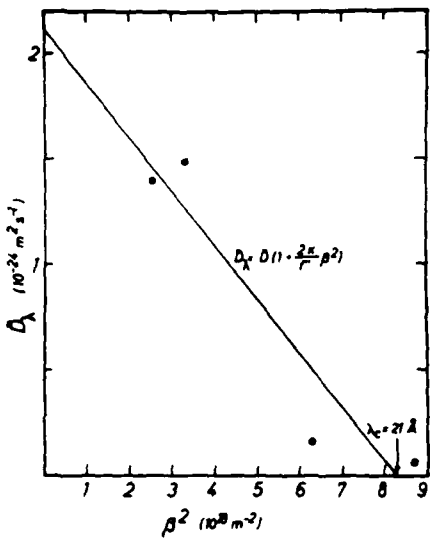

Figure 3 : Wavelength dependence of the interdiffusivity in an amorphous $(Pd_{85}Si_{15})_{50}(Fe_{85}B_{15})_{50}$ modulated film annealed at 250°C. After Cammarata and Green [16].

- 6 kJ . mole^{-1} [28], and ordered phases occur in the crystalline state. A self-consistent calculation of ΔU from Figure 3 and equations (11) and (12), however, is not possible. It is probably necessary to extend the calculation of κ beyond the nearest neighbor approximation [29].

The scaling relation between diffusivity, D, and viscosity, η, [30]is:

$$\eta D = \frac{kT}{L} \tag{16}$$

where L is a characteristic length. In the liquid state, and around the glass transition temperature, L = 3*a, corresponding to the Stokes-Einstein relation. To use the value of Figure 4, it is necessary to correct for the chemical driving force [24] :

$$\tilde{D} = D \frac{c(1-c)\, f''\tilde{V}}{RT} \tag{17}$$

or, with c = 0.5 and the regular solution approximation of equation (11) $\tilde{D} = D\,(1 - 2\Delta U/RT)$. Using the calculated value ΔU = - 6 kJ.mole [28], this gives : $\tilde{D}$ = 3.8 D. Combined with earlier results on the viscosity [15,16, 27], this gives in equation (16) : L = 0.06 a. This is still 150 times smaller than the Stokes-Einstein value, but closer to it than an earlier estimate without the driving force correction [16]. It should, of course, be kept in mind that this analysis is only approximate, since there is insufficient information to take possible chemical effects of the metalloids, B and Si, on the interdiffusion of Fe and Pd into account.

COARSENING

In a phase separating system inside the spinodal (see Figure 1a), a composition modulation of sufficiently large wavelength ($\lambda > \lambda_c$) grows. This has been observed in modulated films of the Au-Ni [10] and Cu-Ni [12, 13] systems. The modulation amplitude continuous to increase until it

reaches the equilibrium composition at the annealing temperature. At the same time, "squaring" of the composition profile occurs, and continues until each point is at one of the two equilibrium compositions, except for the interfaces, which must have a finite width due to the gradient energy [21]. This final state in the evolution of a growing modulation is called a "stationary state". It is clear that the evolution towards this state can no longer be described by the linear diffusion equations (6), since κ, f" and M can only be assumed constant if the amplitude, A, is small. For larger amplitudes, the composition dependence of f can be taken into account with a composition dependent diffusion coefficient, which is usually done by a Taylor expansion in $\Delta c = c - c_o$:

$$\tilde{D} = \tilde{D}^o + \tilde{D}' (\Delta c) + \tfrac{1}{2} \tilde{D}'' (\Delta c)^2 \qquad (18)$$

The coefficients are proportional, respectively, to the second, third and fourth derivatives of f, and are therefore related to the spinodal and equilibrium compositions [13]. Analyses based on the resulting non-linear diffusion equation have been made by de Fontaine [31], Cahn [32], Langer [33] and Tsakalakos [12,13,33]. In the non-linear regime, the Fourier components of a composition profile are coupled; as a result, higher harmonics, leading to "squaring" of an initially purely sinusoidal wave and to saturation of growth at a stationary state, are introduced. By fitting the experimentally observed evolution, as a function of annealing time, of the fundamental and the harmonics to the theory, the coefficients in equation (18) can be determined [12,13,35].

The stationary state is still thermodynamically unstable due to its density of interfaces. The free energy can therefore be lowered further by a continuous process of coarsening. Since this process is driven by the surface tension, σ, it is useful to recall Cahn and Hilliard's [21] result for a diffuse interface :

$$\sigma = 2 \frac{f''^2}{f^{IV}} \zeta, \qquad (19)$$

where

$$\zeta = \frac{1}{2} \sqrt{\frac{-\kappa}{f''}} \qquad (20)$$

The width of the interface is 2ζ. In the classical Lifshitz-Slyozov-Wagner theory of Ostwald ripening the coarsening rate of a population of spherical precipitates in the diffusion-limited regime is given by [36] :

$$R^3 - R_o^3 = C_1 \tilde{V} M \sigma t \qquad (21)$$

where R is the average particle size, R_o the initial average particle size, and, C_1 a proportionality constant. Langer [33] has developed a theory for identifying some of the stationary states in one- and three-dimensional spinodally decomposing systems, and has demonstrated this instability. From the rate of decay of these states, he was able to predict the coarsening rate. For a three-dimensional system of spherical particles, he predicts:

$$R^3 - R_o^3 = C_2 f'' \tilde{V} M \zeta t \qquad (22)$$

where C_2 is again a proportionality constant. Taking into account eq. (19), the functional dependence on time and surface tension in equations (21) and (22) are seen to be the same.

For a one-dimensional system, such as the modulated structures consi-

dered here, he has identified as "uniform" coarsening process, illustrated in Figure 4, in which alternating layers of one component thicken and thin down, leading to an eventual doubling of the wavelength. The coarsening rate, expressed as a continuous process, is then :

$$\lambda - \lambda_0 = \frac{\xi}{2} \ln \left(1 - \frac{8f^{-}\bar{V}Mt}{2} e^{-2\lambda_0/\xi}\right) \qquad (23)$$

where λ_0 is the initial wavelength.

A second mechanism for coarsening in modulated films involves the motion of fault lines (i.e. edges of missing planes), as observed in the coarsening of lamellar eutectics. As illustrated on Figure 5, the half plane recedes by diffusion of atoms from its tip to the thickening adjacent lamellae. A simple analysis of the diffusional flow driven by the difference in curvature between the tip (positive) and the adjacent lamellae (negative), gives for the coarsening rate [37] :

$$\lambda - \lambda_0 = C_3 \rho_f \bar{V} M \sigma t \qquad (24)$$

where C_3 is a geometrical constant, estimated at about 300; ρ_f is the fault line density (i.e. the number of configurations of Figure 5 per unit area).

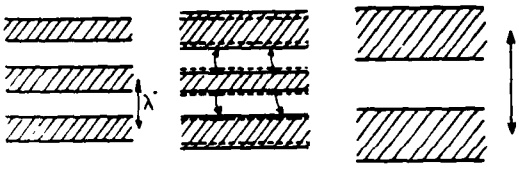

Figure 4 : Successive stages of the uniform coarsening process described by Langer [33].

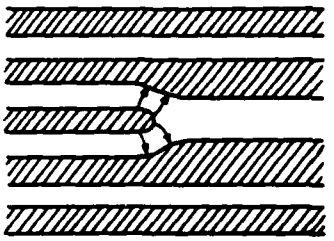

Figure 5 : Schematic diagram of the diffusional flow in the coarsening mechanism governed by a receding fault line. After Graham and Kraft [37].

Although this fault mechanism is likely to dominate the uniform one, due to the higher driving force, it is still interesting to compare equations (23) and (24). The linear dependence on time of the fault mechanism is found only approximately in the uniform mechanism of equation (23), and only if $\lambda \gg \xi$, which is the macroscopic limit. The linear proportionality of the coarsening rate, $d\lambda/dt$, with the surface tension found in the fault mechanism, however, does not have a simple equivalent in the uniform mechanism. From equation (23) it is seen that $d\lambda/dt$ indeed increases with ξ (proportional to σ ; equation (19)) in the macroscopic limit ($\lambda \gg \xi$), but not linearly. For short wavelengths ($\lambda < \xi/2$), the coarsening rate, even decreases with increasing ξ, presumably due to increasing overlap between the diffuse interfaces of adjacent layers. It seems likely that the fault mechanism also needs to be corrected in the short wavelength limit ($\lambda \leq \xi$).

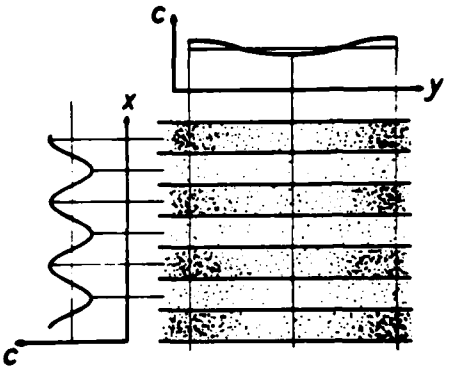

Figure 6 : Schematic diagram of the compositional profile resulting from two orthogonal modulation waves.

In modulated materials of phase separating systems inside the spinodal, one also must consider the possibility of additional phase separation in directions other than these of the original modulation, as illustrated on Figure 6. This situation is different from that usually encountered in spinodal decomposition, where the two orthogonal waves usually have similar amplitudes. In a modulated film, the pre-existence of a large amplitude modulation affects the stability of small waves orthogonal to it. This will be demonstrated below on a simple example.
Consider a two-dimensional superposition, as in Figure 6 :

$$\Delta c = c - c_0 = C_x \cos \beta_x x + C_y \cos \beta_y y \tag{25}$$

The total free energy of the system is given by the two-dimensional equivalent of equation (2) :

$$F = \mathcal{L} \iint [f(c) + \kappa(\vec{\nabla} c)^2] \, dxdy \tag{26}$$

The bulk free energy must have at least one non-parabolic term, for example:

$$f(c) = -\frac{1}{2} A (\Delta c)^2 + \frac{1}{4} B (\Delta c)^4 \tag{27}$$

The total free energy per unit volume is then :

$$F = -\frac{A}{4}(C_x^2 + C_y^2) + \frac{3B}{32}(C_x^4 + C_y^4 + 4C_x^2 C_y^2) + \frac{\kappa}{2}(C_x^2 \beta_x^2 + C_y^2 \beta_y^2) \tag{28}$$

From this equation it is immediately clear that if the amplitudes are small ($C^4 \ll C^2$), or if the free energy is parabolic ($B = 0$, linear diffusion equation), the two waves are independent and have the same stability criterion ($\partial F / \partial C_i < 0$), $\beta^2 < A/2\kappa$, which is identical to the expression derived from equation (10). The case of interest here is : $B \neq 0$, and $C_y \ll C_x$, so that higher powers of C_y can be neglected. The stability criteria for the two waves are now different :

$$\beta_x < (A - \frac{3}{4} B C_x^2)/2\kappa \tag{29}$$

$$\beta_y < (A - \frac{3}{2} B C_x^2)/2\kappa \tag{30}$$

Comparison of equations (29) and (30) shows that the spectrum of new small amplitude orthogonal waves, C_y, is not only more restricted than that of waves forming from a homogeneous solution, but even than that of the large amplitude pre-existing modulations.

A similar qualitative conclusion can be reached from Cahn's non-linear analysis of the later stages of spinodal decomposition [32], in which he derives expressions for the growth rates of coupled orthogonal waves of a particular wavenumber, β, by successive approximation. In the problem of interest here, the spectrum of the first approximation is dominated by a single wave of amplitude C_x. The amplification factors, at $t = 0$, for waves in the $\hat{x}$ and $\hat{y}$ directions in the second approximation are then :

$$R_x = \frac{1}{C_x}\frac{dC_x'}{dt} = R\left[1 + \frac{3}{4}\frac{\tilde{D}''}{\tilde{D}_\lambda} C_x^2\right] \tag{31}$$

$$R_y = \frac{1}{C_y}\frac{dC_y'}{dt} = R\left[1 + \frac{3}{2}\frac{\tilde{D}''}{\tilde{D}_\lambda} C_x^2\right] \tag{32}$$

where C_x' and C_y' are the amplitudes of the waves in Cahn's second approximation, R is the amplification factor in the linear regime (equation (9)), $\tilde{D}_\lambda$ is the interdiffusion coefficient of equation (10) (negative), D'' is the quadratic coefficient in equation (18), which is proportional to $f^{iv} = 68$. Again, the growth rate of the orthogonal wave is only affected in the non-linear regime ($B \neq 0$), and if the original modulation is large. In that case, its growth rate is not only less than in the linear regime, but also less than that of the original modulation.

CONCLUSIONS

Artificial compositionally modulated materials are inherently unstable. The modulation disappears, either by homogenization (in long wavelength ordering systems, in phase separating systems outside the spinodal or for short wavelengths inside the spinodal), or by initial sharpening of the profile to a stationary state (in long wavelength phase separating systems or short wavelength ordering systems) followed by coarsening.

Measurements of the rate of homogenization are a very sensitive method for determining interdiffusion coefficients. For crystalline materials, the method allows determination of the lattice diffusion coefficient at very low homologous temperatures. For metallic glasses, it permits time dependent measurements of $\tilde{D}$, which are essential to take into account structural relaxation.

Two coarsening mechanisms, a uniform one, and one governed by the motion of fault lines, have been discussed. Further investigation into the coarsening rate of the fault mechanism for wavelengths on the order of the interface thickness seems desirable. The presence of an initial, large amplitude modulation wave stabilizes the structure, through the non-linear effects in the diffusion equation, against the growth of certain waves orthogonal to the original one. A full analytic or numerical treatment of this question, especially taking into account crystal anisotropy, would be of interest.

ACKNOWLEDGEMENTS

It is a pleasure to acknowledge much collaboration and discussion on this subject with Lindsay Greer, especially during the writing of ref. 20. I am also grateful to the Metallurgy Department of the University of Leuven for their hospitality during the writing of the paper. Our research in this area is currently supported by the Office of Naval Research, under contract

number N00014-85-K-0023.

REFERENCES

1. J. DuMond and J.P. Youtz, J. Appl. Phys., 11, 357 (1940).
2. H.E. Cook and J.E. Hilliard, J. Appl. Phys., 40, 2191 (1969).
3. L.L. Chang, L. Esaki, W.E. Howard, R. Ludeke and G. Schul, J. Vac. Sci. Technol., 10, 655 (1973).
4. A.H. Eltoukhy and J.E. Greene, Appl. Phys. Lett., 33, 343 (1978).
5. M.P. Rosenblum, F. Spaepen and D. Turnbull, Appl. Phys. Lett., 37, 184 (1980).
6. B. Abeles and T. Tiedje, Phys. Rev. Lett., 51, 2003 (1983).
7. A. Guinier, "X-ray diffraction", Freeman, San Francisco, (1963), p. 169, 209-212.
8. D. de Fontaine, in "Local atomic arrangements studied by X-ray diffraction", ed. by J.B. Cohen and J.E. Hilliard, Gordon Briach, N.Y. (1966).
9. E.M. Philofsky and J.E. Hilliard, J. Appl. Phys., 40, 2198 (1969).
10. W.M.-C. Yang, Ph.D. Thesis, Northwestern Univ., (1979).
11. W.M. Paulson and J.E. Hilliard, J. Appl. Phys., 48, 2117 (1977).
12. T. Tsakalakos, Thin Sol. Films, 86, 79 (1981).
13. T. Tsakalakos, Scripta Met., 15, 225 (1981).
14. M.P. Rosenblum, Ph.D. Thesis, Harvard University (1979).
15. A.L. Greer, C.-J. Lin and F. Spaepen, Proc. 4th Int. Conf. on Rapidly Quenched Metals, ed. by T. Masumoto and K. Suzuki, Jap. Inst. Metals, Sendai, (1982), p. 567.
16. R.C. Cammarata and A.L. Greer, J. Non-Cryst. Solids, 61/62, 889 (1984).
17. R.C. Cammarata, unpublished results.
18. R.E. Somekh and A.L. Greer, unpublished results.
19. G.B. Stephenson, J. Non Cryst. Solids, 66, 393 (1984).
20. A.L. Greer and F. Spaepen, in "Synthetic Modulated Structure Materials", ed. by L.L. Chang and B.C. Giessen, Academic, New York, in press.
21. J.W. Cahn and J.E. Hilliard, J. Chem. Phys., 28, 258 (1958).
22. J.W. Cahn, Acta Met., 9, 795 (1961).
23. J.W. Cahn, Acta Met., 10, 179 (1962).
24. J.E. Hilliard, in "Phase Transformations", ed. by H.I. Aaronson, Am. Soc. Metals, Metals Park, Ohio, (1970), p. 497-560.
25. J.W. Cahn, Trans. Met. Soc. AIME, 242, 166 (1968).
26. H.E. Cook, D. de Fontaine, and J.E. Hilliard, Acta Met., 17, 765 (1969).
27. A.I. Taub and F. Spaepen, Acta Met., 28, 1781 (1980).
28. A.R. Miedema, Philips Tech. Rev., 36, 217 (1976).
29. A.L. Greer, private communication.
30. F. Spaepen, in "Physics of Defects", Les Houches Lectures XXXV, ed. by Balian et al., North-Holland, Amsterdam, (1981), p. 133.
31. D. de Fontaine, Ph.D. Thesis, Northwestern University (1967); some results also in ref. 24.
32. J.W. Cahn, Acta Met., 14, 1685 (1966).
33. J.S. Langer, Ann. Physics, 65, 53 (1971).
34. T. Tsakalakos, Ph.D. Thesis, Northwestern University (1977).
35. R.M. Fleming, D.B. McWhan, A.C. Gossard, W. Wiegmann and R.A. Logan, J. Appl. Phys., 51, 357 (1980).
36. C. Wagner, Z. Elektrochem., 65, 581 (1961).
37. L.D. Graham and R.W. Kraft, Trans. Met. Soc. AIME, 236, 94 (1966).

Interdiffusion in Si/Ge amorphous multilayer films

S. M. Prokes and F. Spaepen
Division of Applied Sciences, Harvard University, 29 Oxford Street, Cambridge, Massachusetts 02138

(Received 12 April 1985; accepted for publication 10 May 1985)

Multilayered or compositionally modulated amorphous Si/amorphous Ge films with a repeat length of 5.83 nm have been fabricated using ion beam sputtering. The interdiffusion coefficient D_λ was determined by measuring the intensity of the x-ray satellite arising from the modulation as a function of annealing time. The interdiffusion was found to be relatively rapid, in that it could be measured easily without crystallization occurring. The temperature dependence in the range 550–630 K is described by $D_\lambda = 1.07 \times 10^{-10} \exp(-1.6\ \text{eV/kT})\ \text{m}^2\text{s}^{-1}$.

Atomic diffusion in amorphous semiconductors has not been studied until very recently, and the only data available so far are for impurity diffusion.[1] The diffusion of the covalent random network formers themselves, i.e., the Si or Ge atoms, has so far not been investigated. The main problem here is the thermal stability of the amorphous phase. Above about 700 K for amorphous Ge[2,3] and 900 K for amorphous Si,[3] rapid crystallization sets in. It is therefore *a priori* not at all clear that the diffusion rate of the network atoms should ever be fast enough to be measurable.

The most sensitive technique available for measuring diffusivities makes use of multilayered or compositionally modulated films with a repeat length of a few nanometers. By monitoring the intensity of the x-ray reflection resulting from the modulation as a function of annealing time, interdiffusivities as low as $10^{-27}\ \text{m}^2\text{s}^{-1}$ can be measured. This technique, originally developed for crystalline materials,[4–6] has been used successfully to measure diffusivities in amorphous metals.[7–9] Since it is nondestructive, the technique allows successive measurements on the same sample. This is particularly important in amorphous materials, which exhibit structural relaxation that affects all physical properties, and, in particular, the atomic transport coefficients.[6,8,10] The compositionally modulated film technique can therefore be used to monitor the extent of structural relaxation, and to ascertain that measurements as a function of temperature are carried out under isoconfigurational conditions (i.e., with negligible relaxation).

Multilayered films of (hydrogenated) amorphous Si (*a*-Si) and amorphous Ge (*a*-Ge) have been made before,[11] but so far they have not been used for the study of interdiffusion.

The *a*-Si/*a*-Ge compositionally modulated films used in the present study were prepared using an ion beam sputtering system consisting of an ion gun that sputters from alternating, motor driven targets.[12] The thickness of the layers is controlled by a monitoring crystal. The 1-μm-thick films were sputtered onto a copper substrate and had an average composition of $Si_{50}Ge_{50}$, as determined by electron microprobe analysis. The layer repeat length (or compositional wavelength), determined by x-ray diffraction, was 5.83 nm. Figure 1 shows x-ray traces of the first, second, and third order satellites about the (000) reflection. The measured full width at half-maximum for the first-order satellite was $\Delta(2\theta) = 0.09°$ for CrK_α radiation. This corresponds to a 7% variation in the layer thickness during deposition. The samples were examined by transmission electron microscopy, and, from the diffraction pattern and dark-field images, were found to be completely amorphous. Differential scanning calorimetry (DSC) measurements were also performed to check the thermal stability. At a scan rate of 40 K/min, two exothermic peaks were observed. The first, at 800 K, corresponds to the amorphous-to-crystalline transition of Ge; the second, starting at 880 K, can be attributed to the crystallization of *a*-Si. These crystallization temperatures of *a*-Ge and *a*-Si are consistent with the results of Chen and Turnbull[2] and Donovan *et al.*[3]

One film was annealed in a furnace that was first evacuated and then backfilled with helium. The temperature was monitored using a thermocouple connected to a chart recorder, so that corrections for the heat-up time could be made. After each anneal, the decay of the x-ray satellites was determined on a G.E. horizontal diffractometer, using CrK_α radiation. X-ray scans were also made at appropriate values of 2θ to detect possible crystallization during the anneals. No crystalline Bragg peaks were observed during the entire experiment. Figure 2 shows the decay of the integrated intensity of the first-order satellite as a function of annealing time for different temperatures. The decay of the intensity, I, is related to the interdiffusion coefficient D_λ by[5]

$$\frac{d}{dt}\ln\left(\frac{I}{I_0}\right) = \frac{-8\pi^2}{\lambda^2} D_\lambda, \tag{1}$$

where λ is the composition modulation wavelength and I_0 is the initial intensity.

The initial anneal was performed at 630 K, and further measurements were made at progressively lower tempera-

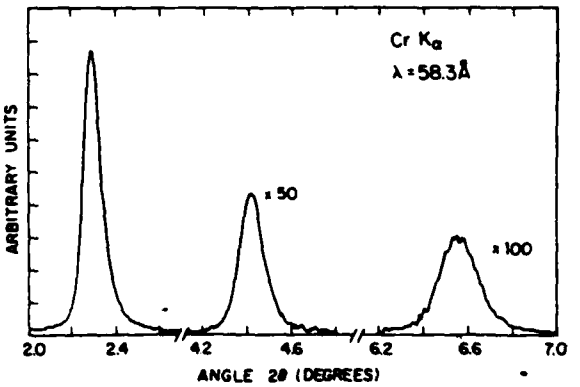

FIG. 1. X-ray diffractometer scan (CrK_α radiation) of an *a*-Si/*a*-Ge compositionally modulated film with a repeat length of 5.83 nm.

 0003-6951/85/150234-03$01.00

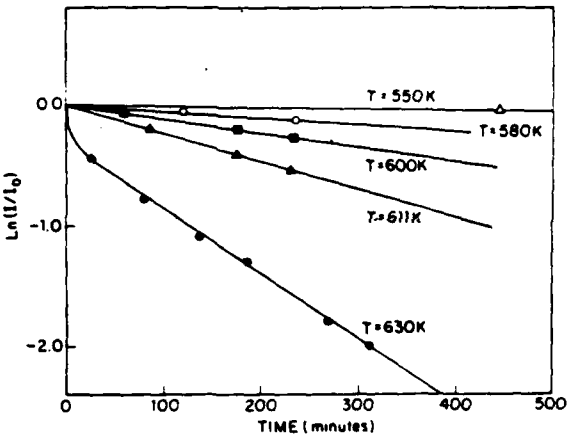

FIG. 2. Decay of the intensity of the first satellite as a function of annealing time and temperature.

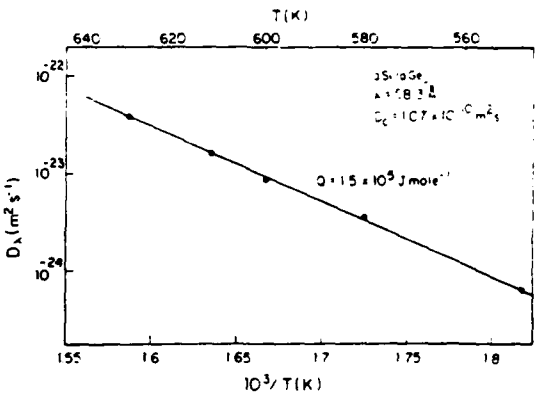

FIG. 3. Temperature dependence of the interdiffusivity, D_λ.

tures. As discussed by Greer *et al.*,[8] this procedure, combined with a sufficiently long first anneal, establishes isoconfigurational conditions. A plot of the logarithm of normalized intensity versus time for each anneal is shown in Fig. 2. The interdiffusivity at 630 K was measured again following the series of experiments at lower temperatures, and was found to be only 5% lower than the first value. Such reproducibility demonstrates that the measurements are, in fact, isoconfigurational.

A small amount of nonlinearity, most likely caused by structural relaxation,[8] was seen during the early part of the first anneal at 630 K, after which the decay became linear. The interdiffusivity D_λ was determined for each temperature from the slopes of the lines on Fig. 2 according to Eq. (1).

The results are listed in Table I. As illustrated by Fig. 3, the temperature dependence can be described by Arrhenius law with an activation energy of 1.5×10^5 J mole^{-1} and a pre-exponential factor $D_0 = 1.07 \times 10^{-10}$ m^2 s^{-1}. An extrapolation of the data to 700 K yields $D_\lambda = 6.8 \times 10^{-22}$ m^2 s^{-1}, in good agreement with the range 10^{-21}–10^{-22} m^2 s^{-1}, estimated by Tsuei from the observation, by means of the resistivity change, of the crystallization of an *a*-Si/*a*-Ge multilayer.[13]

The interdiffusivities measured in the present work are remarkably high, which is, of course, the reason why they could be measured without any crystallization occurring. This is also apparent from a comparison with diffusion in crystals. At 630 K, the interdiffusivity in the amorphous phase is 3.86×10^{-23} m^2 s^{-1}, whereas the only relevant crystalline data available give a diffusivity of Ge in crystalline Si or Ge, extrapolated to this temperature, of only 4.35×10^{-37} m^2 s^{-1} and 5.3×10^{-30} m^2 s^{-1}, respectively.[14,15] The high interdiffusivity measured in the amorphous phase is certainly not a result of short-circuit diffusion along grain boundaries or dislocations. Even in crystals, it is the bulk diffusivity that governs the interdiffusion in modulated films, due to the modulation repeat length being much shorter than the distance between lattice defects. The only effective short-circuit paths identified in crystalline modulated films are *moving* grain boundaries,[5] and they are clearly not found in amorphous materials.

TABLE I. Interdiffusivity D_λ in an *a*-Si/*a*-Ge compositionally modulated film with a repeat length of 5.83 nm

T(K)	D_λ (m^{2}s^{-1})
630	3.86×10^{-23}
611	1.64×10^{-23}
600	8.3×10^{-24}
580	3.66×10^{-24}
550	6.6×10^{-25}

The microscopic mechanism for the diffusion of the network atoms is as yet unclear. The low pre-exponential could result from the diffusion being governed by pre-existing, nonequilibrium defects, such as broken bonds, that are relaxing out very slowly. Since a normal pre-exponential for substitutional diffusion would be about 10^{-4}–10^{-5} m^2 s^{-1}, a defect concentration of about 10^{-5} per atom would be required. The activation energy is close to the Ge–Ge bond energy; it is conceivable that a diffusive jump of Si atoms in Ge, which presumably dominates the interdiffusion process, requires the breaking of an extra matrix bond next to the pre-existing defect.

Before the diffusion mechanism can be positively identified, a considerable number of factors must be taken into account. (i) The gradient energy, which is known to be important for modulations on the scale considered here,[5,9,16] leads to dependence of the interdiffusivity on the modulation repeat length. In the present work, however, the repeat length is fairly large, and the reported interdiffusivities D_λ are therefore probably close to the bulk value. (ii) Coherency strains, which are known to affect the interdiffusion in crystals,[17] are probably not present in the as-prepared films; they may become more significant, however, in the course of the interdiffusion.[18] (iii) The composition dependence of the interdiffusion and the attendant asymmetry in the concentration profile must be considered. (iv) Effects of certain impurities cannot be ruled out entirely at this stage. (v) The kinetics of structural relaxation, and its relation to the pre-existing defects must be characterized in detail. The last two factors can be elucidated by variations in the method of preparation.

At the present stage, it can certainly be stated that a new diffusion process in amorphous semiconductors has been identified, which is remarkably fast, so that it can be measured easily without risk of crystallization of the material.

We thank Professor D. Turnbull for his continuous interest and his comments, R. C. Cammarata for useful discussions and help with the experiments, J. L. Bell for assistance with the sputtering, and F. N. Molea for assistance with the x-ray measurements. This work has been supported by the Office of Naval Research under contract No. N00014-85-K-0023.

[1]R. G. Elliman, J.M. Gibson, D. C. Jacobson, J. M. Poate, and J. S. Williams, Appl. Phys. Lett. **46**, 478 (1985), and references therein.
[2]H. S. Chen and D. Turnbull, J. Appl. Phys. **40**, 4214 (1969).
[3]E. P. Donovan, F. Spaepen, D. Turnbull, J. M. Poate, and D. C. Jacobson, J. Appl. Phys. **57**, 1795 (1985).
[4]J. DuMond and J. P. Youtz, J. Appl. Phys. **11**, 357 (1940).
[5]H. E. Cook and J. E. Hilliard, J. Appl. Phys. **40**, 2191 (1969).
[6]A. L. Greer and F. Spaepen, "Synthetic Modulated Structure Materials," in *Treatise on Materials Science and Technology*, edited by L. Chang and B. C. Giessen (Academic, New York, to be published).
[7]M. P. Rosenblum, F. Spaepen, and D. Turnbull, Appl. Phys. Lett. **37**, 184 (1980).
[8]A. L. Greer, C. J. Lin, and F. Spaepen, *Proceedings of the 4th International Conference on Rapidly Quenched Metals*, edited by T. Masumoto and K. Suzuki (Japan Institute of Metals, Sendai, 1982), p. 567.
[9]R. C. Cammarata and A. L. Greer, J. Non-Cryst. Solids **61/62**, 889 (1984).
[10]A. L. Greer, J. Non-Cryst. Solids **61/62**, 737 (1984).
[11]B. Abeles and T. Tiedje, Phys. Rev. Lett. **51**, 2003 (1983).
[12]F. Spaepen, A. L. Greer, K. F. Kelton, and J. L. Bell, Rev. Sci. Instrum. (in press).
[13]C. Tsuei (private communication).
[14]W. Frank, U. Gösele, H. Mehrer, and A. Seeger, in *Diffusion in Crystalline Solids*, edited by G. E. Murch and A. S. Nowick (Academic, New York, to be published).
[15]A. M. Brown and M. F. Ashby, Acta Metall. **28**, 1085 (1980).
[16]J. W. Cahn and J. E. Hilliard, J. Chem. Phys. **28**, 258 (1958).
[17]J. W. Cahn, Acta Metall. **9**, 795 (1961).
[18]G. B. Stephenson, J. Non-Cryst. Solids **66**, 393 (1984).

 0003-6951/85/150236-03$01.00

THE SUPERMODULUS EFFECT IN COMPOSITIONALLY MODULATED THIN FILMS

R. C. Cammarata*
Division of Applied Sciences
Harvard University
Cambridge, Massachusetts 02138

Introduction

The discovery of the supermodulus effect in highly textured compositionally modulated metallic thin films was made by Hilliard and coworkers (1) at Northwestern University, and most of the subsequent experimental work has been done there (2-9). The biaxial moduli of Au-Ni (1), Cu-Pd (1,2), Cu-Ni (2,3), and Ag-Pd (4,5) films, as measured by the bulge test method, all showed a single peak enhancement of between 100-300% for a composition wavelength around 20 Å, while the biaxial modulus of Cu-Au (4,5) showed no such increase. Baral et al. (6-8) reported a similar enhancement in the flexural modulus, and a bimodal enhancement in Young's modulus and the shear modulus C_{66} (with the 3-axis perpendicular to the plane of the film). The enhancement reported for the flexural modulus of Cu-Ni is shown schematically in Fig. 1.

Some attempts to duplicate the above results have been unsuccessful (9,10), though Testardi et al. (11) saw an enhancement in Young's modulus for a 16 Å wavelength film of Cu-Ni, and Jankowski and Tsakalakos (12) measured a bimodal enhancement of Young's modulus in Cu-NiFe films. A decrease in the C_{44} shear modulus for Cu-Nb (13) and Mo-Ni (14) thin films has been reported by Kueny et al. at the Argonne National Laboratories.

Theoretical attempts to explain the supermodulus effect have been based primarily on either Fermi surface-Brillouin zone interactions or coherency strain phenomena. This article will critically review the current theoretical and experimental understanding of the supermodulus effect, and suggest avenues for further study.

Theoretical Models

The major theoretical attempts to explain the supermodulus effect can be classified as models in which the elastic constants are affected by the presence of either: (a) a Brillouin zone created by the composition modulation which interacts with the Fermi surface, causing a dramatic change in the electronic structure of the film; or (b) the relatively large coherency strains characteristic of textured modulated films, which introduce higher order elastic effects. Any complete theory of the supermodulus effect must be able to account for the magnitude of the rather large enhancements (or dehancements) of the elastic constants, and also show why the effect only occurs near a composition wavelength of 20 Å. In his recent review, Clapp (15) summarily dismissed the theory based on the coherency strain effects, and concentrated on the theories involving the Fermi surface-Brillouin zone interaction, which he claimed were the only ones to make a serious attempt to explain the supermodulus effect. However, in light of experimental and theoretical work that has appeared since his article was presented, there are some major difficulties with the Fermi surface-Brillouin zone interaction theories, and the model based on coherency strain effects must be considered to be on at least an equal footing.

Fermi Surface-Brillouin Zone Interaction Theories

The idea of an interaction of the Fermi surface with a Brillouin zone manifesting itself in the structure and properties of solids is one that dates back to the Jones theory of alloying (16), and is found in various forms throughout solid state physics. In almost every case the effect was originally described in terms of second order perturbation theory, and the same has

*Current address: Department of Materials Science and Engineering, Massachusetts Institute of Technology, Cambridge, Massachusetts 02139.

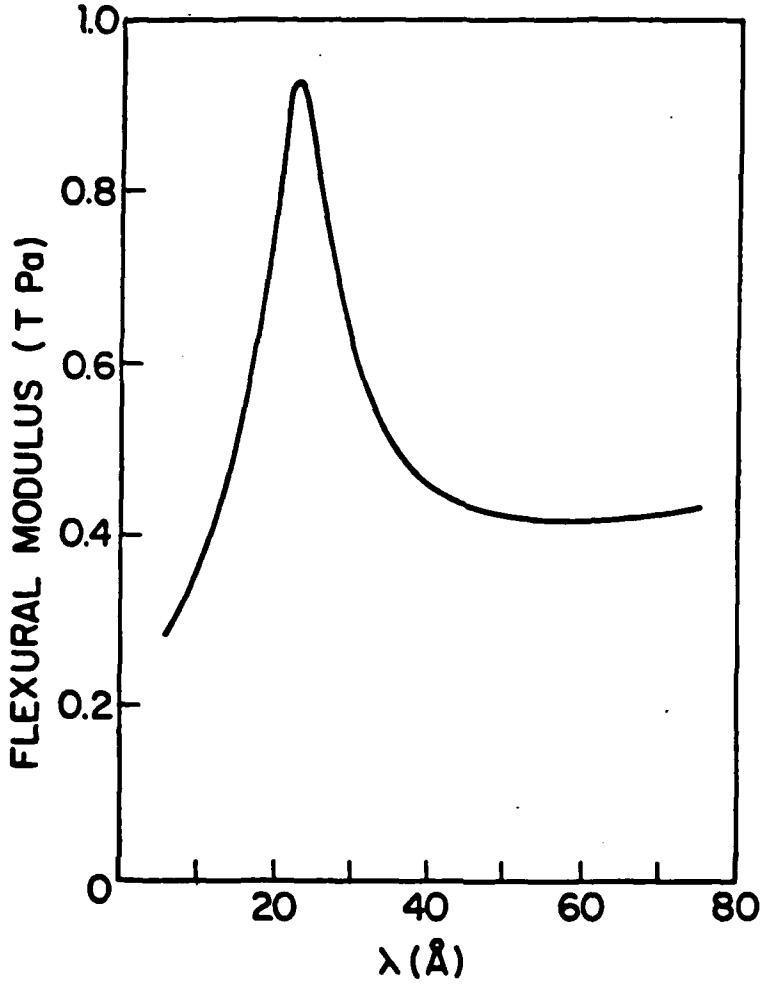

FIG.1 The flexural modulus as a function of composition modulation wavelength, reported for Cu-Ni (6-8).

been done for the supermodulus theories. It should be pointed out that the validity of second order perturbation theory as it has been applied in these cases, as well as the correctness of accepted ideas concerning the Fermi surface-Brillouin zone interaction (FSBZI) in general, have been called into question (17).

The enhancement mechanism of the FSBZI is generally proposed in the following way. A composition modulation with a wavevector $\vec{q}$ creates artificial Brillouin zones at $1/2\ (\vec{k}\pm\vec{q})$, where $\vec{k}$ is a reciprocal lattice vector. Assuming that one of these artificial zones touches a part of the Fermi surface that is not in contact with a Brillouin zone in the absence of a modulation, the change in electronic band structure due to this critical contact could cause the total energy of a modulated film to decrease relative to a homogeneous one. This energy stabilization will be lost if the modulated foil is strained such that a detachment of the Fermi surface from the artificial Brillouin zone occurs. This detachment will manifest itself in a stiffer crystal compared to one without the composition modulation.

Purdes (18) was the first to suggest that if the part of the Fermi surface that experienced the critical contact was flat, a pseudopotential calculation of the band structure energy would predict an energy stabilization. Henein (4) showed that if effects due to screening are taken into account, an enhancement in the elastic constants is predicted due to singularities in the electron dielectric function. A similar explanation has been used to discuss Kohn anomalies in phonon dispersion curves of some elements (19). Though Henein only considered the case of a

Fermi sphere making tangential contact with an artificial Brillouin zone, an enhancement would be expected for any Fermi surface topology. Wu (20) has pointed out an enhancement could also be caused by singularities in the screened ion-ion interaction, and that the closer the modulation is to being sinusoidal, the greater this contribution becomes.

The major success that has been claimed for these FSBZI theories is that λ_c, the wavelength of the composition modulation that causes critical contact, is the wavelength where the enhancement is found experimentally. However, given the error involved in the experimental determination of Fermi surfaces, this success may be overstated. Taking the Cu-Ni system as an example, Henein (4) and Wu (20) calculated the wavelength necessary for critical contact (which is independent of the actual cause of the energy stabilization). They each used a different Fermi surface, obtained from contradictory experimental investigations (21,22). As a result, they each had critical contact occurring at very different places on the Fermi surface. Despite these totally different approaches, they both obtained a wavelength of critical contact close to 20 Å. This suggests that, given the general uncertainties in Fermi surface measurements, together with the supermodulus effect occurring at about the same wavelength independent of the alloy, any agreement between experiment and the FSBZI theories concerning λ_c is probably fortuitous.

There appears to be a difficulty with the FSBZI theories as formulated by Purdes (18) and Henein (4), where the interacting artificial Brillouin zone planes are parallel to the original (111) planes, in explaining the enhancement found in the C_{66} shear modulus of Cu-Ni. Consider a cartesian coordinate system with the 3-axis perpendicular to the plane of the film and the 1- and 2-axes in the plane of the film. If U represents the excess energy density created by a FSBZI, any enhancement δC_{66} in the elastic stiffness C_{66} is given by

$$\delta C_{66} = \left(\frac{\partial^2 U}{\partial \epsilon_6^2}\right)_{\epsilon_6=0}$$

where ϵ_6 is the shear strain in the plane perpendicular to the 3-axis. This means that ϵ_6 must cause a detachment of the Fermi surface from the artificial Brillouin zone for there to be an enhancement. This detachment could be caused by the strain changing the volume of the film, thereby changing the Fermi vector, and/or by the strain changing the wavelength of the modulation, thereby changing the reciprocal lattice vector of the Brillouin zone created by the modulation. Since no volume change accompanies a shear strain, and since the shear strain ϵ_6 only involves the 1- and 2- directions, the contact between the Fermi surface and the artificial Brillouin zone remains unaffected.

Based on the above argument, it seems that no enhancement would be expected in the shear modulus C_{66}. As mentioned in the introduction, Baral measured an enhancement in C_{66} on the same order as the other elastic moduli. Of course this discrepancy may be due to the simplicity of the model, and a more detailed treatment could possibly remedy the situation. Nevertheless, it is disturbing that inclusion of higher order effects in the theory is necessary in order to explain an enhancement in C_{66} that is not needed for the other moduli.

It is possible to argue within the framework of the FSBZI theories that no enhancement would be expected for the Cu-Au system (20,23). It is not easy, however, to explain the observed decrease in the modulus C_{44} observed in Cu-Nb and Mo-Ni foils. If one extends Purdes' and Henein's theories, an enhancement in this elastic constant would be expected for systems that have a FSBZI (24). Since Wu's theory is very sensitive to his choice of parameters, it is difficult to give a precise description of the prediction his model would give; however, it appears that a general calculation would give both an enhancement and a dehancement for different wavelength regimes (24). (This enhancement/dehancement behavior is a feature common to all calculations made by Wu (20).) Kueny et al. (13) suggested that an alternative FSBZI mechanism may be involved in these systems, though no detailed treatment was given.

It should be pointed out that unlike the foils that displayed enhancements, in which both types of layers were composed of *f.c.c.* metals, the films that showed a dehancement were made up of alternating layers of *b.c.c.* and *f.c.c.* materials. As Baral has suggested (6), the electronic interactions in films with immiscible components (such as Cu-Nb and Mo-Ni) may be significantly different from the films that have displayed an increase in the elastic moduli. Thus, the simple FSBZI picture may not be sophisticated enough to account for these differences.

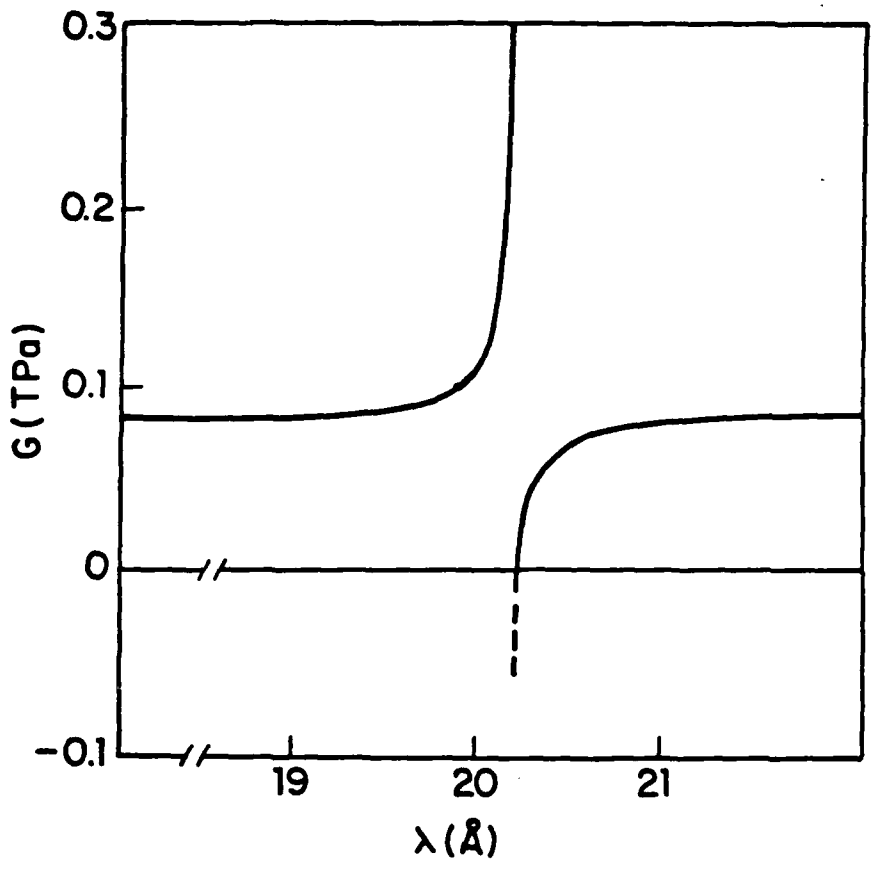

FIG.2 The shear modulus G as a function of composition modulation wavelength, as calculated by Henein (4).

When Henein (4) performed a complete pseudopotential calculation for the enhancement of a shear modulus G (in a different coordinate system than was used above) in order to explain the supermodulus effect he observed in Ag-Pd films, he obtained a result shown schematically in Fig. 2. The behavior of the curve comes from the second derivative (with respect to the modulation wavelength) of the Lindhard screening dielectric function, which contains a logarithmic singularity. As Henein pointed out, a negative shear modulus as obtained in Fig. 2 is a thermodynamic impossibility. He argued that since the wavelength range where the modulus was negative was calculated to be 2×10^{-3} nm, a value of little physical significance, that portion of the figure could be ignored. However, a similar argument could also be made to ignore the enhancement part of the figure. The reason the wavelength range is so small, is because the Lindhard dielectric function contains the very weak logarithmic singular point. If screening dielectric functions with stronger singularities are used, the range of wavelengths that display a negative shear modulus will be large enough that they can no longer be dismissed, and this result must be considered a fundamental difficulty of the theory. A negative shear modulus is also a possibility in Wu's model.

Though the FSBZI theories are presently the most popular explanations for the supermodulus effect, it still remains to be shown that these models are able to account for the rather large enhancements in the various moduli that have been observed. The singularities on which these theories are based come from the fact that the calculations are done for 0 K, thereby assuming a perfectly sharp Fermi surface. A crucial test of the validity of the FSBZI theories is if they still predict large enhancements when a calculation is made for a finite temperature.

If they do, however, there is then another problem to be resolved. Clapp (15) made the observation that the types of model based on an energy stabilization due to Fermi surface-Brillouin

zone interactions such as have been discussed for the supermodulus effect have in the past been used to explain the stability of certain structures. If it is assumed that the FSBZI interaction indeed causes large enough energy changes to explain the supermodulus effect, then it would be expected that a modulated film with this large energy stabilization should be thermodynamically more stable than a homogeneous one. However, all the foils that have been displayed an enhanced modulus interdiffuse when subjected to low temperature anneals, and convert into homogeneous composition films. It is possible, therefore, to argue that the FSBZI theories are doomed from the start: either they will predict an effect too small to account for the enhancements observed in the elastic moduli, or they will predict a large enough stabilizing effect that is at odds with the observation that the films are unstable to homogenization.

Coherency Strain Model

The other major theory that has been proposed to explain the supermodulus effect is based on changes in the properties of compositionally modulated thin films due to coherency strain effects (CSE). The general idea is that the large coherency strains present in modulated films displace the atoms from their equilibrium positions to such an extent that they are no longer within the "Hookean" part of atomic potential. As a result, higher order elastic constants are necessary to describe the elastic behavior of the film. These higher (third) order elastic constants are manifested as enhancements in the standard second order elastic constants.

Clapp (15) has argued that contributions to the elastic moduli due to higher elastic constants could not even come close to accounting for the experimentally observed enhancements in modulated films. However, Jankowski and Tsakalakos (J-T) have recently calculated such contributions in copper, for which the third order elastic constants are known, and showed that a large increase is possible (25,26). They stated that, since the symmetry of a film subjected to a biaxial stress state (due to coherency strains) is changed, any calculation of elastic moduli must be done using the elastic constants dictated by the symmetry of the stressed state. Unlike calculations in cubic symmetry, which gave no enhancements (4,25,26), J-T obtained large changes in the (100) biaxial modulus in copper determined in the tetragonal symmetry of its stressed state. For example, if a copper layer was subjected to a 3% compressive biaxial strain due to coherency, the biaxial modulus would almost double (25,26).

J-T also used the pseudopotential approach of Thomas (39) to determine the third order contributions to the elastic constants of copper. The largest contribution to the elastic moduli due to the anharmonic nature of the interatomic potential comes from the repulsive ion-core overlap energy. Using a suitable expression for this overlap energy, such as a Born-Mayer potential, any enhancements in the elastic constants can be calculated from the second derivative of the overlap energy with respect to the appropriate strains. J-T made such calculation and obtained enhancements in the (100) biaxial modulus similar to those obtained from the measured third order elastic constants when computed for tetragonal symmetry. Calculations using the Born-Mayer potentials for gold and silver also showed large enhancements.

Because the sign of the contribution from the CSE depends on whether the stresses in the layers due to the coherency strains are compressive or tensile (since the contribution comes from third order terms), such a theory can potentially explain both the increases and decreases in elastic moduli that have been seen experimentally. J-T also discussed that despite the partial cancellation due to the opposite sign contributions, there will still be a large enough net effect to explain the observed magnitude of the supermodulus effect. However, it appears that there may be some difficulty in explaining why no enhancement occurs in the Cu-Au system.

The major difficulty with the CSE theory is in explaining why the enhancements are found only for an intermediate range of modulation wavelengths, or more precisely, why the effect is suppressed for large and small wavelengths. J-T pointed out that for long modulation wavelengths, it is energetically more favorable for the film to have misfit dislocations at the interfaces than to retain the strain energy associated with coherency. If the film does become incoherent at long wavelengths, it will lose any effects due to coherency, such as enhancements in the moduli. Such an argument has been used to interpret anomalous diffusion behavior in Cu-Pd (27). However, Gyorgy et al. (28) have inferred from their magnetic measurements that Cu-Ni remains coherent for wavelengths between 16 and 120 Å.

The arguments of J-T concerning the lack of a supermodulus effect at small wavelengths are not very convincing. They state that because of ubiquitous interdiffusion during fabrication,

small wavelength films do not have as large a composition modulation amplitude as longer wavelength films will. However, even if the experimental measurements are corrected to take into account any differences in amplitude, there is still no evidence of any enhancement, as was in fact shown by Makalakos for Cu-Ni (2) and J-T for Cu-NiFe (12). The other argument concerning small wavelength films offered by J-T (26) is not very clear: "... the effective layer thickness for coherency strains across each interface is about three to five atomic dimensions. Thus the maximum value of the *biaxial* modulus occurs in a 0.8-1.2 nm layer thickness (their italics)." This seems to imply that modulated films are coherent only within a certain interfacial region, while the rest of the film has an intraplanar lattice parameter that can vary along the modulation direction (presumably without the introduction of dislocations, which J-T have reserved for longer wavelength films). Allowing films to vary their intraplanar lattice parameter in this way would create astronomically large shear strains, and cannot be accepted as a realistic situation.

Two other points concerning small wavelength films are perhaps worth mentioning. Since small wavelength (on the order of two atomic spacings) films mimic ordered structures while longer wavelength films simulate phase separated structures, properties of modulated thin films, such as the elastic moduli, may reflect these differences. Also, an elastic "gradient" energy term has been predicted to be an important contribution for small wavelength foils (29), and may affect the effective elastic moduli measured in these films.

In summary, at its current stage of development, the CSE theory seems to be able to account for the magnitude of both the increases and decreases in the elastic moduli that have been experimentally determined. It is also consistent with the observation that the modulated films with the supermodulus effect are not stable with respect to films that have a homogeneous composition. What has yet to be shown is that the theory can adequately explain why the supermodulus effect is only seen for a limited range of composition modulation wavelength. Despite this limitation, however, it cannot be considered at this time any less valid than the FSBZI theories.

Since all the theories of supermodulus thus far presented are based on quantum mechanical calculations, it will be necessary to consider the problem beyond the simple pseudopotential approach that has been used. For example, it has been shown that coherency strains have a very large effect on the density of states near the Fermi level (30). Though efforts are underway to develop a quantum mechanically more sophisticated formalism for band structure determination in modulated films (31,32), no attempts have been made to use them to calculate enhanced moduli. Obviously, a lot more work is necessary before it can be claimed that even a partial theoretical understanding of the supermodulus effect has been attained.

Experimental Aspects of the Supermodulus Effect

Several methods have been developed to measure various elastic moduli of modulated films (1,2,6,9,13). Though certain problems may exist with some of these tests, as will be discussed below, it nevertheless would be desirable to employ all of them on the systems discussed in the introduction, since such a catalogue would give a clearer empirical understanding of the supermodulus effect. Though it is much more easily said than done, it would also be worthwhile to develop a procedure to measure Poisson's ratio ν in the plane of the film. This modulus must exhibit a rather unusual dependence on the wavelength in Cu-Ni in order to explain the bimodal enhancement of Young's modulus E and the single peak enhancements of the biaxial $\{E/(1-\nu)\}$ and the flexural $\{E/(1-\nu)^2\}$ moduli (2,3,6-8). Baral (6) attempted to measure Poisson's ratio in the thickness direction, and though his results were inconclusive, they suggested that this modulus was negative for some composition wavelengths.

Itozaki (9) has pointed out certain difficulties associated with the bulge test, and claimed that apparent enhancements observed in the biaxial modulus of various modulated films were just experimental artifacts. Baral (6) has shown, however, that despite these objections the supermodulus results were still valid. One problem with the bulge test that was not addressed was that nonlinear effects may become important for very small amounts of deflection, given the thinness of the films. This possibility has not been incorporated in the analysis employed to interpret bulge test results. A similar objection can be raised with the vibrating reed method used to measure the flexural modulus (24). Though this question is important for precise modulus determination, it probably does not invalidate the general enhanced modulus effects that have been observed, since the supermodulus effect has demonstrated a wavelength dependence that could not be explained by systematic errors introduced by any nonlinear aspects of the method of measurement.

A more important issue concerns what modulus is actually measured in the vibrating reed test (24). This method involves measuring the resonant frequency of a film shaped as a reed, clamped at one end. The modulus corresponding to this configuration depends on the aspect ratio of the reed (width over length). As this ratio goes to zero, Young's modulus is measured; as the ratio goes to infinity, the flexural modulus is measured. For finite size reeds, St. Venant's principle suggests that the transition from the one modulus to the other occurs when the aspect ratio is close to unity, though this would be valid only for isotropic reeds, which modulated films obviously are not. The foils measured by Baral were generally five times longer than they were wide (33), a ratio that suggests that he actually measured Young's modulus rather than the flexural modulus as he reported. If this is true, there is a major discrepancy between the results for Cu-Ni obtained by Baral in the vibrating reed configuration and those he reported as Young's modulus, measured in a microtensile apparatus.

One area of experimental investigation that requires more attention than it has received is the relationship between the supermodulus effect and the structural nature of the modulated films. For example, it would be interesting to see some electron microscopy done on the interfaces in modulated films, such as Cu-Ni, of various wavelengths in order to directly observe the possible existence of misfit dislocations. Such a grid of dislocations would signify a loss of coherency that is predicted to occur in long wavelength films, and might explain changes in moduli, as was discussed before. Structural studies on the systems that have shown a modulus dehancement are also worth pursuing. It was reported (14) that the Mo-Ni films in which a decrease in shear modulus was observed also showed evidence of a crystalline to amorphous transition as a function of modulation wavelength. This transition should be characterized in more detail, since it gives an obvious reason for the abrupt decrease in the shear modulus. Also, the 35% decrease in the shear modulus reported for Cu-Nb films (13) (no precise value was given for the decrease in the Mo-Ni foils) is characteristic of a crystalline to amorphous phase change in metals (34).

It has been observed that plastic properties of artificially modulated structures have shown a correlation with enhanced moduli. For example, Baral et al. (6-8) found an enhancement in the microhardness of Cu-Ni modulated films that correlated with their vibrating reed results. To some extent this is to be expected, since elementary dislocation theory predicts the energy of edge and screw dislocations to be proportional to the biaxial and Young's moduli, respectively. Improved plastic properties of modulated thin films in fact were predicted by Koehler (35) before the discovery of the supermodulus effect, based on models that considered only impediments to dislocation creation and motion, and not on any mechanism to enhance the elastic moduli.

Bevk et al. (36-38) studied the elastic and plastic properties of composites made up of Nb filaments with diameters between 50 and 3000 Å in a Cu matrix. These composites would be predicted to display enhanced resistance to plastic flow, according to Koehler's theory. Along with an increase in the yield and tensile strengths, an enhancement in the Young's modulus by a factor of two to three was observed. This is quite intriguing, since this behavior is essentially identical with that seen in Cu-Ni modulated films. As mentioned above, Koehler's theory did not involve any change in the elastic moduli, and the theories of supermodulus effect do not seem to apply, since the widths of the filaments are much larger than the modulation wavelengths where the enhanced moduli have been observed in modulated films. Cohen and Bevk (37) suggested that the enhancement in their composites may originate from thermally induced elastic strains at the matrix-filament interface. Further experimental work is warranted concerning the existence of enhanced moduli in composites, the effect being interesting in its own right, but also because it might shed more light on the nature of the supermodulus effect in compositionally modulated thin films.

Acknowledgements

The author thanks D. Baral for useful discussions, and F. Spaepen and A.L. Greer for a critical reading of the manuscript. This work was supported by the Office of Naval Research under contract N00014-85-K-0023 and by the National Science Foundation under contract DMR83-16979.

References

1. W.M.C. Yang, T. Tsakalakos, and J.E. Hilliard, J. Appl. Phys. 48, 876 (1977).
2. T. Tsakalakos, Ph.D. Thesis, Northwestern University (1977).
3. T. Tsakalakos and J.E. Hilliard, J. Appl. Phys. 54, 734 (1983).

4. G. Henein, Ph.D. Thesis, Northwestern University (1979).
5. G. Henein and J.E. Hilliard, J. Appl. Phys. 54, 728 (1983).
6. D. Baral, Ph.D. Thesis, Northwestern University (1983).
7. D. Baral, J.B. Ketterson, and J.E. Hilliard, in Modulated Structure Materials, NATO ASI Series, Applied Sciences, ed. T. Tsakalakos, Martinus Nijhoff, Dordrecht, p. 465 (1984).
8. D. Baral, J.B. Ketterson, and J.E. Hilliard, J. Appl. Phys. 57, 1076 (1985).
9. H. Itozaki, Ph.D. Thesis, Northwestern University (1982).
10. B.S. Berry and W.C. Pritchett, Thin Solid Films 33, 19 (1976).
11. L.R. Testardi, R.H. Willens, J.T. Krause, D.B. McWhan, and S. Nakahara, J. Appl. Phys. 52, 510 (1981).
12. A.F. Jankowski and T. Tsakalakos, in Layered Structures, Epitaxy, and Interfaces, Materials Research Society Symposia Proceedings, ed. J.M. Gibson and L.R. Dawson, Materials Research Society, Pittsburgh, Pennsylvania, Vol. 37, p. 529 (1985).
13. A. Kueny, M. Grimsditch, K. Miyano, I. Banerjee, C.M. Falco, and I.K. Schuller, Phys. Rev. Lett. 48, 166 (1982).
14. M.R. Khan, C.S.L. Chun, G.P. Felcher, M. Grimsditch, A. Kueny, C.M. Falco, and I.K. Schuller, Phys. Rev. B27, 7186 (1982).
15. P.C. Clapp, in ref. 7, p. 455.
16. H. Jones, Proc. Roy. Soc. A144, 225 (1934).
17. V. Heine and D. Weaire, in Solid State Physics, ed. H. Ehrenreich, F. Seitz, and D. Turnbull, Academic Press, NY, Vol. 24, p. 250 (1970).
18. A. Purdes, Ph.D. Thesis, Northwestern University (1976).
19. W.A. Harrison, Pseudopotentials in the Theory of Metals, W.A. Benjamin, Reading, MA (1966).
20. T.-B. Wu, J. Appl. Phys. 53, 5265 (1982).
21. M. Hasegawa, T. Suzuki, and M. Hiribayashi, J. Phys. Soc. Japan 37, 85 (1974).
22. S. Nanao, K. Kuribayashi, S. Taniwaga, and M. Doyamam, Phys. Lett. 38A, 489 (1972).
23. W.E. Pickett, J. Phys. F: Met. Phys. 12, 2195 (1982).
24. R.C. Cammarata, Ph.D. Thesis, Harvard University (1985).
25. T. Tsakalakos and A.F. Jankowski, in ref. 7, p. 387.
26. A.F. Jankowski and T. Tsakalakos, J. Phys. F: Met. Phys. 15, 1279 (1985).
27. A. Philofsky, Ph.D. Thesis, Northwestern University (1968).
28. E.M. Gyorgy, J.F. Dillon, D.B. McWhan, L.W. Rupp, L.R. Testardi, and P.J. Flanders, Phys. Rev. Lett. 45, 57 (1980).
29. H.E. Cook and D. DeFontaine, Acta Metall. 19, 607 (1971).
30. A.J. Freeman, J. Xu, and T. Jarlborg, J. Mag. & Mag. Mat. 31-34, 909 (1983).
31. A. Gonis and N.K. Flevaris, Phys. Rev. B25, 7544 (1982).
32. A.L. Yeyati, N.V. Cohan, and M. Weissmann, Phys. Rev. B31, 873 (1985).
33. D. Baral, private communication.
34. D. Weaire, M.F. Ashby, J. Logan, and M.J. Weins, Acta Metall. 19, 779 (1971).
35. J.S. Koehler, Phys. Rev. B2, 547 (1970).
36. J. Bevk, J.P. Harbison, and J.L. Bell, J. Appl. Phys. 49, 6031 (1978).
37. D.E. Cohen and J. Bevk, Appl. Phys. Lett. 39, 595 (1981).
38. J. Bevk, Ann. Rev. Mater. Sci. 13, 319 (1983).
39. J.F. Thomas, Jr., Phys. Rev. B1, 2385 (1973).

BASIC DISTRIBUTION LIST

Technical and Summary Reports December 1982

Organization	Codes
Defense Documentation Center Cameron Station Alexandria, VA 22314	12
Office of Naval Research Department of the Navy 800 N. Quincy Street Arlington, VA 22217 Attn: Code 431	3
Naval Research Laboratory Washington, DC 20375 ATTN: Codes 6000 6300 2627	1 1 1
Naval Air Development Center Code 606 Warminster, PA 18974 ATTN: Dr. J. DeLuccia	1
Commanding Officer Naval Surface Weapons Center White Oak Laboratory Silver Spring, MD 20910 ATTN: Library	1
Naval Oceans Systems Center San Diego, CA 92132 ATTN: Library	1
Naval Postgraduate School Monterey, CA 93940 ATTN: Mechanical Engineering Department	1
Naval Air Systems Command Washington, DC 20360 ATTN: Code 31A Code 5304B	1 1
Naval Sea System Command Washington, DC 20362 ATTN: Code 05R	1

Organization	Copies
Naval Air Propulsion Test Center Trenton, NJ 08628 ATTN: Library	1
Naval Construction Battallion Civil Engineering Laboratory Port Hueneme, CA 93043 ATTN: Materials Division	1
Naval Electronics Laboratory San Diego, CA 92152 ATTN: Electron Materials Sciences Division	1
Naval Missile Center Materials Consultant Code 3312-1 Point Mugu, CA 92041	1
Commander David W. Taylor Naval Ship Research and Development Center Bethesda, MD 20084	1
Naval Underwater System Center Newport, RI 02840 ATTN: Library	1
Naval Weapons Center China Lake, CA 93555 ATTN: Library	1
NASA Lewis Research Center 21000 Brookpark Road Cleveland, OH 44135 ATTN: Library	1
National Bureau of Standards Washington, DC 20234 ATTN: Metals Science and Standards Division Ceramics Glass and Solid State Science Division Fracture and Deformation Div.	1 1 1

Naval Facilities Engineering Command
Alexandria, VA 22331
ATTN: Code 03 1

Scientific Advisor
Commandant of the Marine Corps
Washington, DC 20380
ATTN: Code AX 1

Army Research Office
P. O. Box 12211
Triangle Park, NC 27709
ATTN: Metallurgy & Ceramics Program 1

Army Materials and Mechanics Research Center
Watertown, MA 02172
ATTN: Research Programs Office

Air Force Office of Scientific Research/NE
Building 410
Bolling Air Force Base
Washington, DC 20332
ATTN: Electronics & Materials Science Directorate 1

NASA Headquarters
Washington, DC 20546
ATTN: Code RRM 1

Defense Metals and Ceramics Information Center
Battelle Memorial Institute
505 King Avenue
Columbus, OH 43201 1

Metals and Ceramics Division
Oak Ridge National Laboratory
P.O. Box X
Oak Ridge, TN 37380 1

Los Alamos Scientific Laboratory
P.O. Box 1663
Los Alamos, NM 87544
ATTN: Report Librarian 1

Argonne National Laboratory
Metallurgy Division
P.O. Box 229
Lemont, IL 60439 1

Brookhaven National Laboratory
Technical Information Division
Upton, Long Island
New York 11973
ATTN: Research Library 1

Library
Building 50, Room 134
Lawrence Radiation Laboratory
Berkeley, CA 1

Send ONE COPY to each unless otherwise indicated.

END
FILMED
4-86
DTIC